Applied Radiation and Isotopes 200 (2023) 110986

Contents lists available at ScienceDirect

Applied Radiation and Isotopes

journal homepage: www.elsevier.com/locate/apradiso

Activity standardisation of ^{177}Lu

Youcef Nedjadi *, Frédéric Juget, M. Teresa Durán, Laurent Desorgher, François Bochud, Claude Bailat

Institut de Radiophysique, Lausanne, Switzerland

ARTICLE INFO

Keywords:
Activity standardisation
4πβ-4πγ coincidence counting
Plastic scintillation
TDCR
^{177}Lu

ABSTRACT

^{177}Lu decays through low-energy β⁻- and γ-emissions in addition to conversion and Auger electrons. To support the use of this radiopharmaceutical in Switzerland, a ^{177}Lu solution was standardised using the β-γ coincidence technique, as well as the TDCR method. The solution had no ^{177m}Lu impurity. Primary coincidence measurements, with plastic scintillators for beta detection, were carried out using both analogue and digital electronics. TDCR measurements using only defocusing were also made. Monte Carlo calculations were used to compute the detection efficiency. The coincidence measurements with both analogue and digital electronics are compatible within one standard uncertainty, but they are lower than (and discrepant with) the TDCR measurements. An ampoule of this solution was submitted to the BIPM as a contribution to the *Système International de Référence*.

1. Introduction

We recently reported on the activity standardisation of ^{161}Tb (Nedjadi et al., 2020). Here we turn our attention to its matching alternative for targeted radionuclide therapy: ^{177}Lu. Both these rare-earth nuclides have close half-lives and beta energies, though ^{177}Lu emits less conversion and Auger electrons (Lehenberger et al., 2011; Champion et al., 2016). ^{177}Lu ground state beta transitions to the ground state and three excited states of ^{177}Hf. Energies and emission probabilities of the quanta released in the decay of this nuclide have been recently reviewed (Kellett, 2016).

This work presents the measurements made at IRA-METAS, the designated national metrology institute in Switzerland, to develop a primary activity standard for this radionuclide. Many activity standardisations of this nuclide have been performed (Capogni et al., 2012; Dias et al., 2010; Dryák et al., 2016; Kossert et al., 2012; Rezende et al., 2012; Schötzig et al., 2001; Simpson et al., 2012; Zimmerman et al., 2012). The β-γ coincidence measurements used so far for this nuclide involved either a proportional counter or liquid scintillation for β-detection (Zimmerman et al., 2012). Our coincidence counting standardisation of ^{177}Lu brought to bear plastic scintillation for β-detection. Pulse processing and data acquisition were carried out with both analogue and digital electronics. Back-up measurements with the TDCR method were also carried out. Double and triple coincidence detection efficiencies were computed using Monte Carlo simulations with the Geant4 code coupled with the radioactivity and atomic relaxation modules (Allison et al., 2006, 2016).

An aliquot of the ^{177}Lu solution we standardised was dispatched to the International Bureau of Weights and Measures (BIPM) as part of a contribution to the *Système International de Référence*.

2. Material and methods

The measurements described below were carried out in two steps.

2.1. ^{177}Lu solution and dilutions

^{177}Lu was provided by ITM GmbH. A 2 mL solution was received in an Eppendorf vial, with a nominal activity of 1 GBq on the date of delivery. The solution consisted of 0.1 mol L^{-1} HCl solvent with a Lu^{3+}-ion concentration of 20 μg g^{-1}. The density of the solution was 1.000(7) g cm^{-3}.

An aliquot of 0.65 g from this solution was diluted by a factor of about 40 to prepare a master solution (M177Lu4). Two 3 g aliquots were dispensed into 5 mL IER (Institut d'Électrochimie et de Radiochimie) ampoules for activity measurements in our reference ionisation chamber (CIR). Two BIPM ampoules were each filled with 3.6 mL of this solution, one of which was dispatched to the *BIPM* in Paris after both had been measured in our CIR. Two 3 g aliquots were also transferred into two ISO ampoules for CIR and primary measurements.

* Corresponding author.
E-mail address: youcef.nedjadi@chuv.ch (Y. Nedjadi).

https://doi.org/10.1016/j.apradiso.2023.110986
Received 3 April 2023; Received in revised form 8 August 2023; Accepted 14 August 2023
Available online 16 August 2023

A 1.2 g aliquot of the M177Lu4 solution was diluted by a factor of about 14 to prepare the M177Lu5 solution. The latter was dispensed into two IER ampoules (3 mL each), in order to check the dilution factor at the CIR, and into three ISO ampoules (3 mL each) for primary standardization.

The latter gravimetric dilution factor was first corroborated by ionisation chamber measurements, and later by primary measurements.

2.2. Sources

2.2.1. Plastic scintillation sources

A pycnometer with about 3 g of the diluted M177Lu5 solution was used to deposit weighed drops (~ 70 and 80 mg) of ^{177}Lu onto two plastic scintillators – which had been ultrasonically cleaned earlier – for 4πβ(PS)-γ coincidence measurements. This solution had an activity concentration of about 400 kBq/g when preparing the sources. These UPS-923A plastic scintillators consist of pairs of machined cylindrical pieces which fit into each other to form a single 25 mm height and 25 mm diameter cylinder, inside which there is a centred cylindrical cavity (3 mm × 12 mm) housing the radioactive deposit (Nedjadi et al., 2012). No Ludox was used. After drying, the plastic pairs were bonded together with optical grease.

Two other plastic scintillator sources of the same geometry were also prepared with aliquots (~ 17 and 34 mg) from the M177Lu4 (master) solution. Its activity concentration was about 1 MBq/g when the sources were prepared. In this case, drops of Ludox colloidal silica (Sigma-Aldrich GmbH) with a concentration of 0.03% wt were added to the depositions in order to homogenise the crystallisation process during drying.

2.2.2. Liquid scintillation sources

Aliquots of the M177Lu5 solution were transferred gravimetrically into two sandblasted glass vials using a pycnometer weighed with a Mettler balance traceable to a primary mass standard. These 20 mL low-potassium high-performance borosilicate vials were prefilled with 14.5 mL Ultima Gold cocktail, and topped up with variable volumes of ultrapure water to achieve a 6.5% aqueous fraction, which was found to be necessary for the stability of samples over extended periods (Nedjadi et al., 2016). Each sample was agitated for 2 min with a vortex shaker, and then centrifuged at 15 revolutions per second for 150 s to settle down the liquid on the cap and walls.

Aliquots taken from M177Lu4 were also used to produce two other liquid scintillation sources, using the same procedures described above.

2.2.3. Gamma spectrometry sources

Aliquots of the M177Lu4 and M177Lu5 solutions were used to prepare 20 mL polyethylene vials for HPGe gamma spectrometry. This is one of the geometries for which our HPGe detector underwent a thorough efficiency calibration (Talip et al., 2021). Two M177Lu5 aliquots of about 50 and 75 mg were deposited into two vials pre-filled with about 19.6 mL of lutetium chloride carrier. The samples were then homogenised with a vortex shaker before centrifugation to settle down the matter adhering to the upper parts of the vials. These liquid samples had an activity of about 5 and 7 kBq, respectively, at the start of the impurity measurements.

Two samples were also prepared from the M177Lu4 solution using the same procedure, except that in this case both aliquots had about 35 mg mass and about 14 kBq at the start of their assay.

2.3. Methods

2.3.1. 4πβ(PS)- 4πγ(NaI) coincidence counting

Beta-channel detection consists of a UPS-923A plastic scintillator optically coupled to a selected low-noise one-inch diameter photomultiplier tube. The light-tight thin capsule that encloses this beta detector rests vertically at the bottom of the well of a 120 mm × 120 mm NaI(Tl) gamma ray detector. A source sitting at the bottom of the well interacts with the gamma detector within 99.1% of the full solid angle. This setup is housed at the bottom of a 50-cm-diameter 5-cm-thick cylindrical lead shielding covered with an armour-plated sliding square 6 cm-thick.

Signals were shaped with analogue electronics in both channels. The pulses from the amplifiers were injected into Canberra 2037A single-channel analysers with pulse lockout logic that minimises out-of-channel event deadtime. An in-house digital coincidence selector was used to impose variable non-extending deadtimes and set the coincidence window. A non-extending deadtime of 29 μs was enforced, as a safeguard against PMT afterpulses or scintillator phosphorescence. A resolving time of 1.0 μs was set to let in all coincidences.

The efficiency was varied by low-level discrimination with the beta single-channel analyser. The counting times ranged from 3 to 10 min per efficiency point, depending on the gamma setting and discrimination level, so that the relative standard deviations of the counting rates were all lower than 0.1%. Each of the four sources from the diluted and the mother solutions were measured at three gamma settings.

Digital measurements were also carried out with this system. The beta detector pulses had rise-times in the 5–40 ns range while those from the NaI-well detector were in the 500–600 ns range. Pulses from the beta and gamma detectors were fed into the desktop CAEN DT5725 digitizer, which operates with 8-channels, 14-bit resolution and 250 MS/s sampling rate. Digital Pulse Processing for Pulse Height Analysis (DPP-PHA) algorithms, with the COMPASS software, shape the discretised pulses to access their time and energy information. The timestamps of the pulses are obtained through the zero-crossing of RC-CR^2 signals; the input risetimes were set at 48 and 544 ns for the beta and gamma channels respectively, whilst their trigger holdoff values were set at 96 and 1200 ns, in that order. The energy information was obtained by a simple configuration of trapezoidal pulse processing adapted to the count-rate, with flat top, pole-zero adjusted pulses that are as short as possible to reduce pile-up. The time and energy information was then recorded in list-mode files for off-line analysis. In-house software written in Fortran analyses these records using the pulse-mixing method (Bouchard and Chauvenet, 1999). These measurements were just exploratory as the correct functioning of the digitizer and its software have not been fully validated yet.

2.3.2. 4πβ(PS)-γ($CeBr_3$) coincidence counting

A variation of the set up described in the previous section utilises the same beta detector whilst the gamma detector is substituted for a 51 mm × 51 mm $CeBr_3$ gamma detector. This setup is housed at the bottom of the same lead shielding described above. The four plastic scintillator sources were measured with this system using the DT5725 digitizer.

2.3.3. TDCR counting

This technique was implemented with our TDCR system (Nedjadi et al., 2015) using a MAC3-module (Bouchard and Cassette, 2000) with variable resolving time. The TDCR electronic system was adjusted for an optimal response for ^{177}Lu. The thresholds were set at the valleys of the single-electron responses of the three PMTs. The resolving time was set at 80 ns, and the deadtime at 90 μs. Sources were measured by voltage defocusing varying from 560 to 340 V in 40 V decrements.

2.3.4. Ionisation chamber

The four IER ampoules, two filled with the M177Lu4 solution and two with the M177Lu5 solution and the two BIPM ampoules, filled with the M177Lu4 solution, were measured twice within a week after their preparation. Before each measurement, the ampoule was centrifuged to ensure optimal efficiency and reproducibility. A typical measurement cycle corresponds to the time needed to collect the charge produced by the ionisation in the chamber, and load a given capacitor up to 0.1 V six times. The final ionisation current is given by the mean and its standard deviation obtained from 20 consecutive readings of the current. A

measurement sequence starts with a background measurement using a small 503 pF capacitor. A typical background value is 0.057(2) pA. Two reference ^{137}Cs sources were measured with a larger capacitor (30090 pF) after which the Lutetium ampoules from the M177Lu4 solution were measured with the same capacitor. These measurements were repeated a few days later with a 10040 pF capacitor. For the M177Lu5 dilution, all the ampoules were measured twice with a lower capacitor of 1018 pF. Finally, another background measurement was performed with the small capacitor to complete the sequence. The results were used to calculate a CIR calibration factor for ^{177}Lu. The ratio of the measured currents for the mother and diluted solutions can be compared with the gravimetric dilution factor.

2.3.5. HPGe gamma spectrometry

Spectrometric measurements were carried out with an n-type coaxial HPGe detector calibrated with an efficiency curve obtained using reference sources traceable to international standards. More details about the detector set-up, geometry and the efficiency calibration can be found in (Talip et al., 2021). Three polyethylene vials, two filled with aliquots of the diluted M177Lu5 solution and one from the M177Lu4 solution, were measured to assess gamma-emitting impurities. They were measured sequentially for 40, 113 and 146 live hours respectively, within a two-week window.

3. Results

3.1. Gamma spectrometry

No impurity was observed within the detection limits in the gamma spectra acquired in the three separate measurements. In particular, there was no trace of the ^{177m}Lu isomeric state. No impurity correction was thus required in all the primary and secondary measurements.

3.2. Primary standardisations

3.2.1. 4πβ(LS)-4πγ(NaI) coincidence counting

The ^{177}Lu β-spectrum is presented in Fig. 1. Typically, the β-channel detection efficiency (ε_β) was varied from a maximum of 90% down to around 55%. Count-rates in this channel ranged between 15 and 20 kcps. The beta-background count-rate was 0.3–1.5 cps.

Fig. 2 presents the gamma-ray spectrum. The two most intense gamma emissions at 112.95 and 208.37 keV, respectively, are well separated. There is a well-defined X-ray peak at about 55.8 keV, which is a conflation of several close X-ray emissions. The measurements were made with three-gamma channel settings: a discrimination threshold at 36 keV (before the X-ray peak), a second one at 157 keV (before the 208.37 keV gamma emission), and a window around the 112.95 keV peak. The γ-detection efficiencies for these three situations were around 15%, 9% and 5% correspondingly. These relatively small efficiencies somewhat mirror the low intensity low-energy gamma emissions of this radionuclide.

Fig. 3 shows characteristic efficiency extrapolations at these three gamma regimes. The green diamonds represent the threshold before the second gamma peak, while the blue triangles are for the threshold before the first gamma peak. The red circles depict a window including the first gamma peak. All the fits are linear fits. There is a slight departure from linearity at high efficiencies, which is due to self-absorption in the source. This source was prepared without adding a crystallising agent that produces homogeneous crystals during the drying process. Fig. 4 presents analogous efficiency extrapolations for a source from M177Lu4 where Ludox was added on top of the gravimetric deposition. Here the maximum efficiency is lower than when no Ludox was used but the linearity is maintained throughout the efficiency range. Sets of residuals of the linear fits for a M177Lu4 source are shown, for illustration, in Fig. 5. The relative deviations from linearity range between - 0.3% and 0.3%.

Using sources without Ludox yielded higher efficiencies at the cost of non-linearity while sources with Ludox produced linear efficiency profiles at the expense of the maximum efficiency. The different morphologies of the dried sources explain this difference. For sources dried without Ludox, one sees fine salt crystallites at the centre of the drying drop and much larger crystallites at the periphery. This leads to a minimal self-absorption of the Auger electrons in the centre and a strong one at the periphery. On the other hand, for sources dried with Ludox, there is a homogeneous crystallisation across the radius of the drying drop, with a prevalence of average crystallites centred around Ludox seeds.

As a matter of fact, we do not use the linear fits shown in Figs. 3 and 4

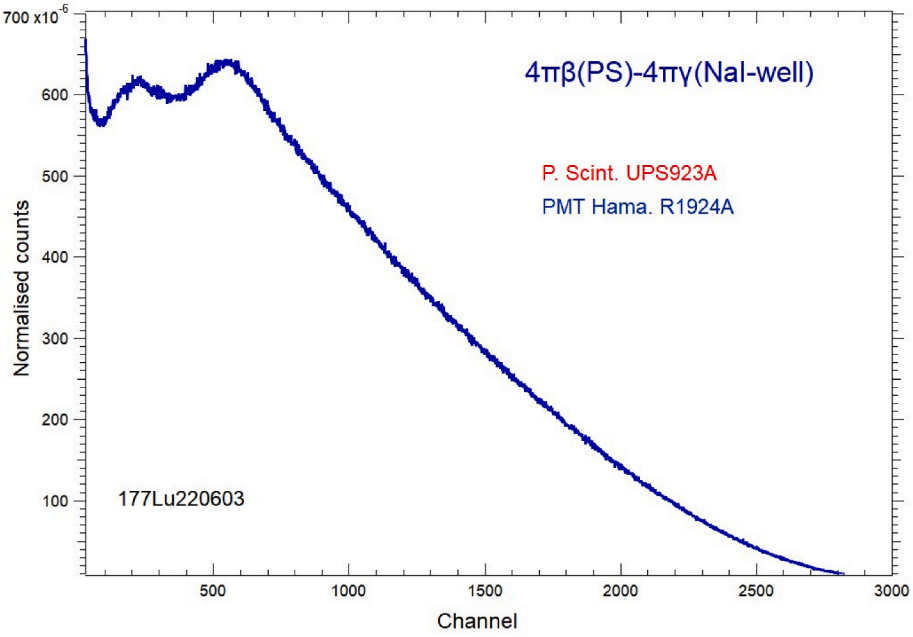

Fig. 1. ^{177}Lu beta singles spectrum obtained with UPS923A plastic scintillator and a 26 mm diameter photomultiplier tube.

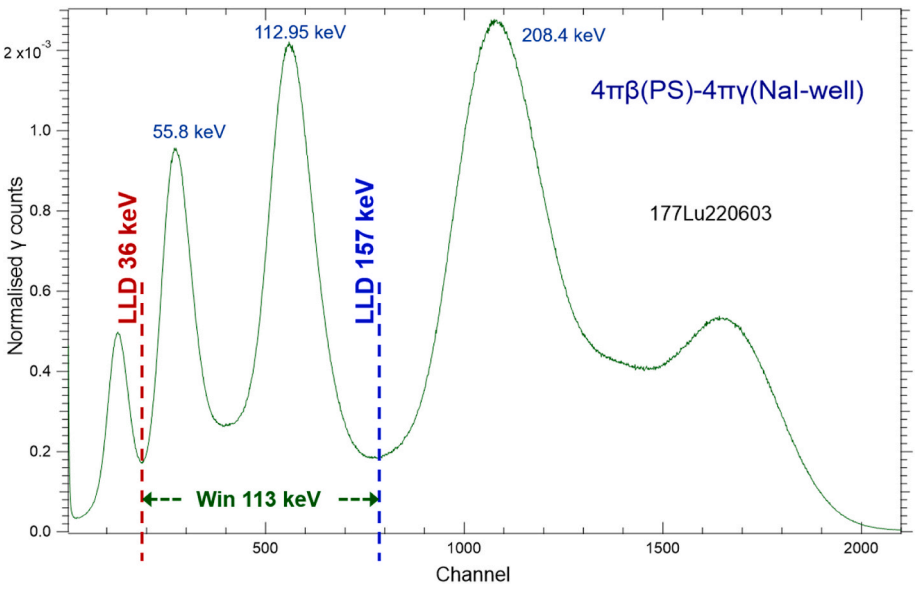

Fig. 2. ^{177}Lu gamma spectrum obtained with a NaI(Tl) well-detector.

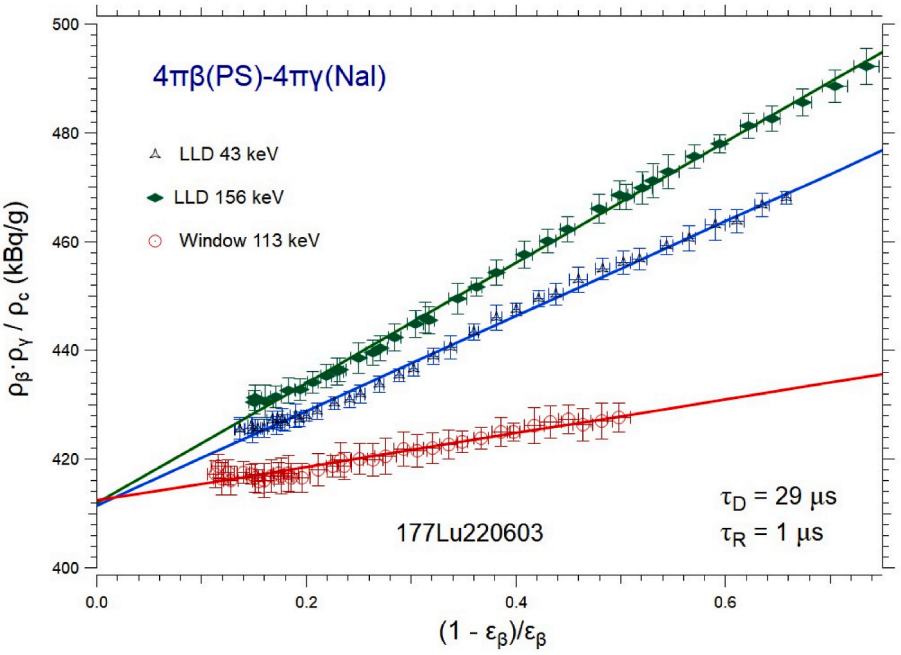

Fig. 3. ^{177}Lu 4πβ(PS)-4πγ(NaI) efficiency extrapolation curves for a plastic source where no Ludox is used. Green diamonds stand for the threshold before the second gamma peak; blue triangles represent a threshold before the first gamma peak, while red circles designate a window including the first gamma peak. The solid lines are linear fits. Horizontal uncertainty bars are standard uncertainties on $(1-\varepsilon_\beta)/\varepsilon_\beta$, while vertical ones are standard uncertainties on $\rho_\beta \cdot \rho_\gamma/\rho_c$.

to determine the radioactive concentration. What we do, instead, is a Monte Carlo fit that takes the uncertainties of both ε_β and $\rho_\beta\rho_\gamma/\rho_c$ into account (Nedjadi et al., 2012). Ten thousand fits are performed by varying stochastically $(1-\varepsilon_\beta)/\varepsilon_\beta$ and $\rho_\beta\rho_\gamma/\rho_c$ within their distributions assumed to be Gaussian. The average of the intercept distribution is then taken to be the actual intercept while the standard deviation of the distribution is estimated to be the intercept uncertainty.

Table 1 compiles the intercepts found for the four sources from the two solutions measured in the three gamma settings. The activities of the M177Lu5 solution are scaled by the gravimetric dilution factor. The degrees of freedom of the twelve efficiency extrapolations range from 31 to 38. The uncertainties listed are the standard deviations of the intercept distributions, as described above. The intercepts for the gamma window have the largest uncertainties, because of the poor gamma detection efficiency. The intercepts of each source for all gamma settings are compatible within 0.02% to 0.6%. The arithmetic mean activities of the two sources from the M177Lu5 agree within 0.3% whereas the equivalent values for the two sources from the M177Lu4 are compatible within 0.5%. The mean M177Lu4 activity concentration differs by 0.34% from the corresponding quantity for M177Lu5 scaled by the gravimetric dilution factor. Combining the extrapolated activities of the four sources measured in the three gamma settings yields an arithmetic average of 5862.76 kBq g^{-1} at the date of reference.

Analytic balances give dilution factors with very small relative standard uncertainty, which provides a stringent test of the internal coherence of standardisations. The ratio of the activity concentration of

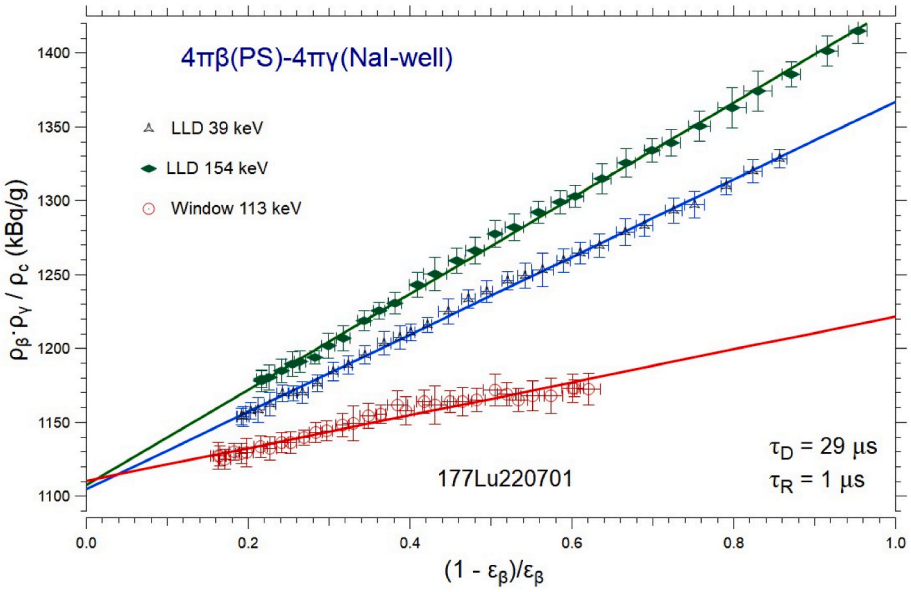

Fig. 4. ^{177}Lu 4πβ(PS)- 4πγ(NaI) efficiency extrapolation curves for a plastic source prepared using Ludox. Green diamonds stand for the threshold before the second gamma peak; blue triangles represent a threshold before the first gamma peak, while red circles designate a window including the first gamma peak. The solid lines are linear fits.

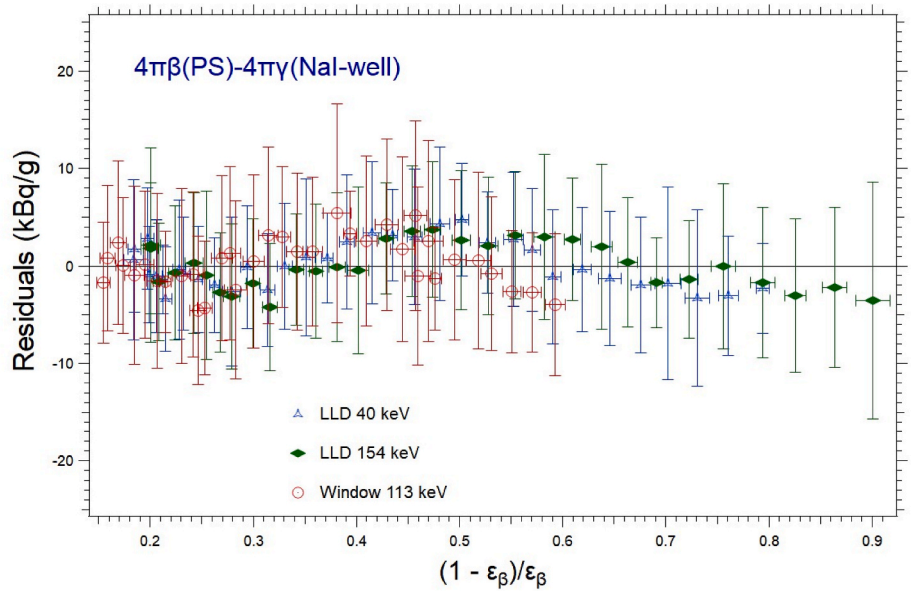

Fig. 5. Residuals of the 4πβ(LS)-4πγ(NaI) efficiency extrapolation lines for a source with Ludox at three gamma settings.

the M177Lu4 solution divided by the unscaled value of the M177Lu5 solution predicted by these coincidence measurements agrees with the gravimetric dilution factor within 0.04%.

Table 2 lays out the uncertainty budget estimated for this coincidence measurement. The background component is $\Delta B_\gamma/R_{\gamma min}$ where ΔB_γ is the maximum deviation of the γ-background rate during the campaign, while $R_{\gamma min}$ is the minimum γ-count-rate measured at the three gamma settings. The half-life uncertainty designates the maximum value of the propagation of the half-life uncertainty to the decay correction factors; the last measurement was used to estimate it. The deadtime uncertainty is estimated as $\Delta\tau \times \rho_\beta$, where $\Delta\tau$ is the uncertainty of the deadtime while ρ_β is an average beta count-rate for the campaign. The resolving time uncertainty was assumed to be $u_{\tau R}\cdot(\rho_{acc}/\rho_{cmax})$ where $u_{\tau R}$ is the relative standard uncertainty of the resolving time, ρ_{acc} is the accidental coincidence count-rate, while ρ_{cmax} is the biggest measured true coincidence count-rate. The weighing uncertainty refers to that of the lightest source of the whole set used. The counting statistics is a typical standard deviation of the mean of $\rho_\beta \bullet \rho_\gamma/\rho_c$. The efficiency extrapolation uncertainty was taken to be the median value of the relative standard deviations of the intercept distributions of all the measurements. Reproducibility, i.e. the relative standard deviation of twelve efficiency-extrapolated activities obtained with four sources from two dilutions, and three gamma settings, was found to be the largest contribution to the uncertainty budget. The combined uncertainty obtained from the quadratic sum of type-A and type-B uncertainties is 0.41% ($k = 1$).

Turning now to the measurement with this same system but using digital electronics, Fig. 6 displays typical efficiency profiles obtained using the 5725 digitizer and processing the list-mode output with the pulse mixing method. The efficiency functions show a distinct non-

Table 1
4πβ(PS)- 4πγ extrapolated intercepts (in kBq/g) for ^{177}Lu. Uncertainties are given with $k = 1$.

Source	γ-setting	Intercept
177Lu220602	LLD 46 keV	5841.9 ± 15.9
	LLD 154 keV	5849.9 ± 17.0
	Win 113 keV	5866.3 ± 19.0
177Lu220603	LLD 43 keV	5867.1 ± 9.8
	LLD 156 keV	5868.1 ± 16.5
	Win 113 keV	5874.0 ± 15.9
M177Lu5 average		**5861.2 ± 5.1**
177Lu220701	LLD 40 keV	5861.3 ± 16.5
	LLD 154 keV	5883.6 ± 20.8
	Win 113 keV	5895.2 ± 20.6
177Lu220702	LLD 41 keV	5839.3 ± 14.5
	LLD 154 keV	5837.8 ± 19.5
	Win 113 keV	5868.7 ± 19.8
M177Lu4 average		**5864.3 ± 9.5**

Table 2
4πβ(PS)- 4πγ coincidence uncertainty budget. Uncertainties are given with $k = 1$.

Uncertainty item	u in %
Background	0.03
Half-life	0.06
Deadtime	0.13
Resolving time	0.03
Timing	0.002
Weighing	0.08
Dilution factor	0.01
Counting statistics	0.10
Efficiency extrapolation	0.25
Sources and gamma settings	0.30
Combined type-A & B uncertainties	0.41

linearity that is absent in the analogue electronics case. This difference is not understood and is being investigated.

Table 3 lists the intercepts obtained for the four sources in various gamma settings. All the intercepts were obtained using the Monte Carlo fitting method. The M177Lu5 activities are normalised with the gravimetric dilution factor. The degrees of freedom are 65 for all the efficiency extrapolations. The uncertainties listed are just the standard deviations of the intercepts. The intercepts of each source for all gamma settings agree within 0.1% to 1.5%. The arithmetic mean activities of the two sources from the M177Lu5 agree within 0.65% whereas the corresponding activities for the two M177Lu4 sources match within 0.45%. The mean M177Lu4 and M177Lu5 activity concentrations agree within 0.03%. Putting together the extrapolated activities obtained with digital electronics yields an arithmetic mean of 5842.63 kBq g^{-1} at the date of reference, which differs by 0.34% from that found using analogue electronics.

3.2.2. *4πβ(PS)-γ(CeBr$_3$) coincidence counting*

A typical CeBr$_3$ gamma spectrum for ^{177}Lu using CAEN DT5725 digital pulse processing and data acquisition is shown in Fig. 7. The β-spectrum produced by the UPS923A plastic scintillator is akin to the one presented in Fig. 1.

An example of efficiency extrapolations using the pulse mixing method is shown in Fig. 8. The β-channel detection efficiency (ε_β) was

Table 3
Digital 4πβ(PS)-4πγ and extrapolated intercepts (in kBq/g) for ^{177}Lu. Uncertainties are given with $k = 1$.

Source	γ-setting	Intercept
177Lu220602	LLD 40 keV	5853.9 ± 3.4
	LLD 84.4 keV	5885.2 ± 5.9
	LLD 157 keV	5839.6 ± 5.5
	Win 113 keV	5862.4 ± 2.3
177Lu220603	LLD 40 keV	5816.2 ± 4.8
	LLD 84.4 keV	5827.7 ± 8.6
	LLD 157 keV	5778.3 ± 8.2
	Win 113 keV	5866.3 ± 2.6
M177Lu5 average		**5841.2 ± 11.9**
177Lu220701	LLD 40 keV	5807.9 ± 9.5
	LLD 157 keV	5817.0 ± 17.7
	Win 113 keV	5863.7 ± 4.1
177Lu220702	LLD 41 keV	5836.7 ± 6.7
	LLD 157 keV	5844.0 ± 13.0
	Win 113 keV	5888.1 ± 3.6
M177Lu4 average		**5842.9 ± 12.1**

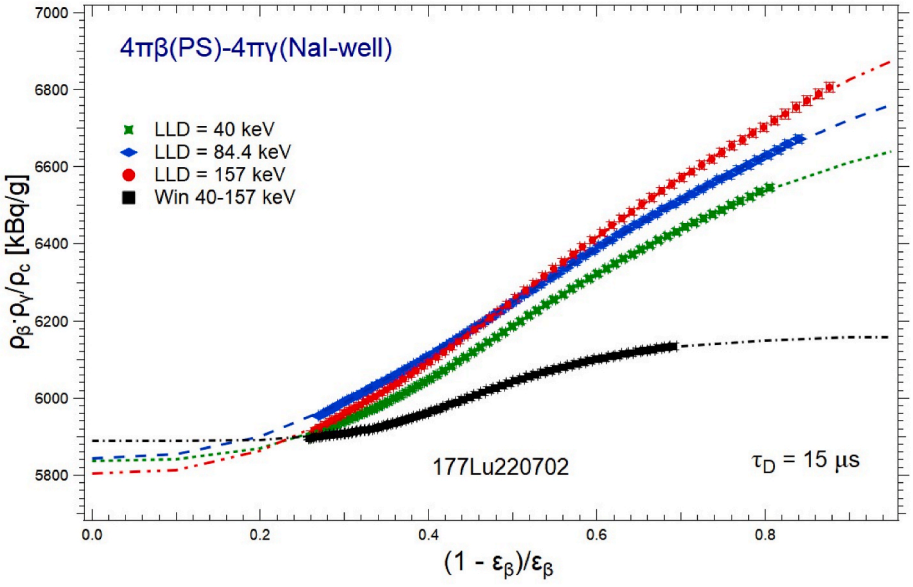

Fig. 6. ^{177}Lu 4πβ(PS)-4πγ(NaI) efficiency extrapolation curves for a plastic source prepared using Ludox obtained with the CAEN DT5725 digitizer. Green stars stand for the threshold before the X-ray peak, blue diamonds represent a threshold before the first gamma peak, red dots depict the threshold before the second gamma peak, while black squares designate a window including the first gamma peak. The various lines are non-linear fits.

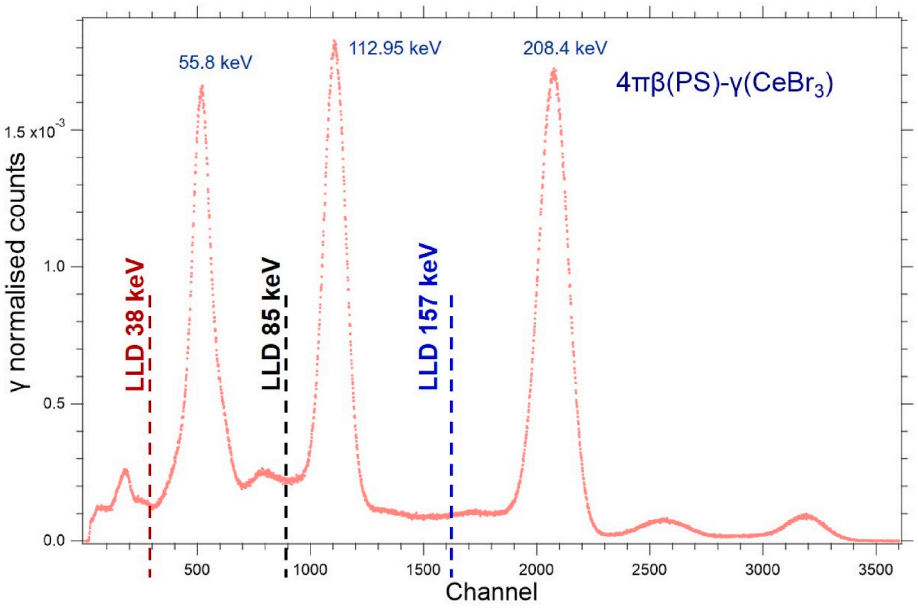

Fig. 7. ^{177}Lu gamma spectrum obtained with a $CeBr_3$-detector.

varied from a maximum of 73% down to around 45% to have data covering at least twice the extrapolation gap. A tentative dead time of 15 μs was used for these computations. Here also a marked departure from linearity is observed. No measurement with this system was made with analogue electronics for comparison, but it seems reasonable to assume that it stems from the CAEN digital pulse processing.

Table 4 reports the intercepts obtained for the four sources from the two solutions measured in many gamma settings. All the efficiency extrapolations involve 65 degrees of freedom. The tabulated uncertainties involve only the standard deviations of the intercepts. They are larger than in 4πβ(PS)-4πγ coincidence counting because the extrapolation gap is larger. The intercepts for different gamma settings cohere within 0.05% to 0.8%. The mean activities of the two M177Lu5 sources are consistent within 0.2%, while those for the two M177Lu4 sources match within 0.4%. The average M177Lu4 activity concentration deviates by 0.3% from that of the M177Lu5 solution normalised by the gravimetric dilution factor. Pooling the extrapolated activities of the four sources measured digitally in the various gamma settings gives an arithmetic average of 5861.69 kBq g^{-1} at the date of reference. This value deviates by 0.02% from the activity concentration obtained with 4πβ(PS)-4πγ coincidence counting with analogue electronics.

3.2.3. *TDCR method*

The efficiencies and activities were computed with an in-house code that takes the PMTs asymmetry and the micelle effect into account (Nedjadi et al., 2017). This program calculates the efficiencies with the stochastic method with the sampled energies (at least a million) of the beta particles or the conversion, Auger and photoelectrons produced in the vial delivered by Geant 4 Monte Carlo simulations including the *Radioactivity* and *Atomic relaxation* modules. Nuclear and atomic data

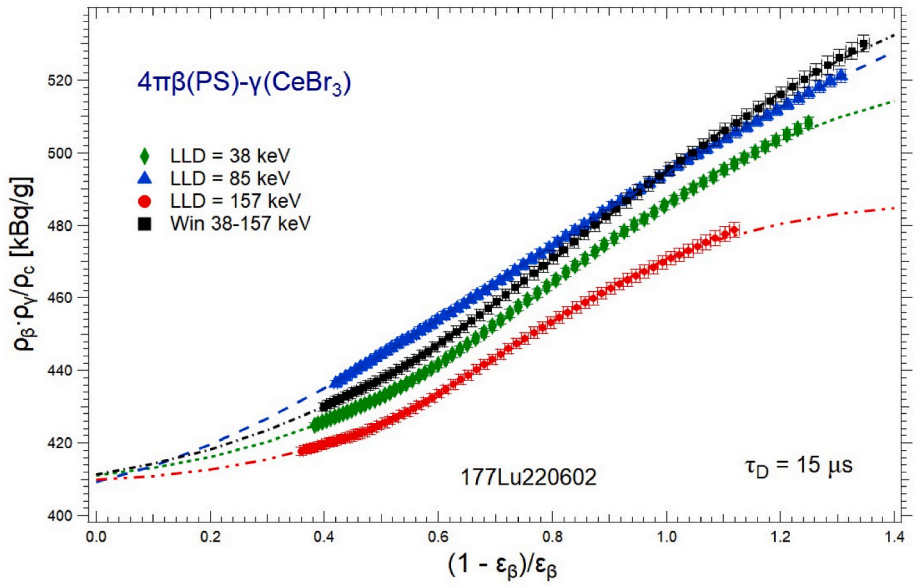

Fig. 8. ^{177}Lu 4πβ(PS)-γ($CeBr_3$) efficiency extrapolation curves for a plastic source prepared using Ludox obtained with the CAEN DT5725 digitizer. Green diamonds represent the threshold before the X-ray peak, blue triangles stand for a threshold before the first gamma peak, red dots show the threshold before the second gamma peak, while black squares denote the window including the first gamma peak. The different lines are non-linear fits.

Table 4
Digital 4πβ(PS)-γ($CeBr_3$) extrapolated intercepts (in kBq/g) for ^{177}Lu. Uncertainties are given with $k = 1$.

Source	γ-setting	Intercept
177Lu220602	LLD 41 keV	5863.0 ± 31.7
	LLD 85 keV	5837.0 ± 67.7
	LLD 155 keV	5845.5 ± 30.0
	Win 113 keV	5867.1 ± 64.4
177Lu220603	LLD 41 keV	5821.2 ± 30.4
	LLD 85 keV	5867.1 ± 71.8
	LLD 155 keV	5858.5 ± 15.3
	Win 113 keV	5826.4 ± 62.9
M177Lu5 average		**5848.2 ± 6.5**
177Lu220701	LLD 42 keV	5827.6 ± 22.9
	LLD 156 keV	5867.3 ± 187.4
	Win 113 keV	5864.4 ± 25.0
177Lu220702	LLD 42 keV	5852.4 ± 16.5
	LLD 156 keV	5895.5 ± 65.3
	Win 113 keV	5886.5 ± 17.1
M177Lu4 average		**5865.6 ± 9.9**

used are from DDEP and ENSDF databases.

For illustration, Fig. 9 displays the variation of the double detection efficiency and that of the activity concentration with the experimental TDCR, for a sandblasted glass scintillation sample from the M177Lu4 solution. The ESTAR stopping powers were used for computing the ionisation quenching function. The detection efficiency typically varies in a narrow range between 0.974 and 0.980. For this sample, the values of T/AB, T/BC, and T/AC were 0.9936, 0.9926 and 0.9938 respectively, at the optimum focusing voltage of 560 V.

Table 5 reports the activity concentrations predicted by the measurements and the model. A *kB* value of 0.0075 cm MeV^{-1} was used. The impact of the ionisation quenching factor *kB* on the activities was found to be moderate. The relative difference between using 0.0075 and 0.012 cm MeV^{-1} for *kB* is about 0.15% for these defocusing measurements. Each listed activity is the average of seven counting points. The average activity of the two sources from M177Lu5 normalised by the dilution factor deviates from the corresponding average of M177Lu4 by 1.1%, which is rather large for this technique. Combining the activity concentrations of the two solutions gives an arithmetic mean of 5970.50 kBq g^{-1} at the date of reference.

The ratio of the activity concentration of the M177Lu4 solution divided by that of the M177Lu5 solution predicted by these TDCR measurements deviate from the gravimetric dilution factor by 1.1%.

Table 5
TDCR ^{177}Lu activities (in kBq/g) for solutions M177Lu4 and M177Lu5. Uncertainties are given with $k = 1$.

Source	Activity conc.
177Lu220621	5913.021 ± 26.026
177Lu220622	5963.462 ± 17.320
M177Lu5 average	**5938.24 ± 25.22**
177Lu220711	5991.930 ± 14.096
177Lu220712	6013.613 ± 11.227
M177Lu4 average	**6002.71 ± 10.84**

The full uncertainty budget is spelt out in Table 6. For the background contribution, one thousand sets of correlated random Gaussian background coincidence counting rates were generated for each counting point. The simulated rates have mean values, standard deviations of the means and covariance matrices in agreement with the measured background rates. Corresponding net counting rates were generated by subtracting the Monte Carlo background rates from the measured gross counting rates. The 10^3 defocusing data sets were then fed into the code that computes the efficiencies and activities. The standard deviation of the distribution of the activities thus obtained was taken as the propagation of the background uncertainty on the activity.

The half-life contribution was computed conservatively as the propagation of the half-life uncertainty to the decay correction factors for the latter measurements. The uncertainties of the intensities of the three main beta branches, 79.44(28) %, 11.52(7) %, and 9.01(29) %

Table 6
TDCR uncertainty budget. Uncertainties are given with $k = 1$.

Uncertainty item	Value in %
Background	0.002
Half-life	0.063
Decay scheme	0.023
kB and Q(E)	0.074
Weighing	0.15
Dilution factor	0.013
Impurity	
Counting statistics	0.226
Reproducibility	0.676
Combined type-A & B uncertainties	0.74

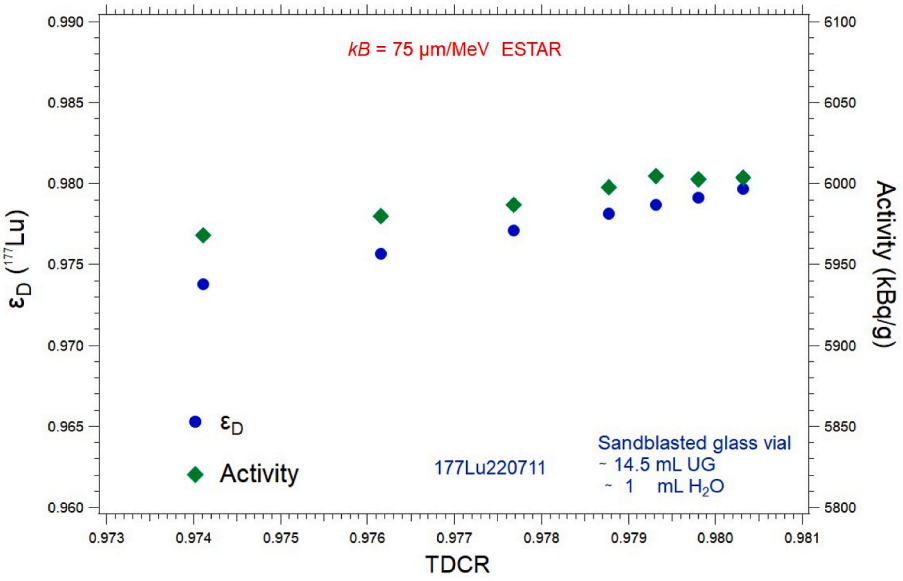

Fig. 9. Variation of the double detection efficiency and the activity concentration with the experimental TDCR for a M177Lu4 sample measured by defocusing between 560 and 340 V in 40 V steps.

(Kellett, 2016), were propagated to get the decay scheme uncertainty. The activities of one sample were calculated using beta intensity sets in which the intensities of these branches took their maximal and minimal values while keeping the sum constant. The decay scheme uncertainty was then estimated as the relative standard deviation of the resulting activities assuming a rectangular distribution.

Since both *kB* and the stopping power correlate through their involvement in the Birks formula, one cannot propagate their uncertainties separately. With regard to the propagation of the uncertainties of the ionisation quenching function and parameter, the procedure used was as follows. Separate sets of $2x10^3$ uniform deviates of *kB* lying between 0.0075 and 0.0120 cm/MeV were randomly generated, assuming a rectangular distribution, and then coupled with five ionisation quenching functions to compute altogether 10^4 activities. Four of these ionisation quenching functions are obtained from the ESTAR stopping powers (Berger, 1993), and those of (Gümüş and Kabadayi, 2010; Tan and Xia, 2012), whereas the fifth is that of (Grau Malonda and Grau Carles, 1999). The relative standard deviation of the 10^4 activities thus generated is about 0.1%.

The counting statistics contribution was estimated using one thousand sets of correlated random Gaussian net coincidence counting rates generated for each of the counting points of a defocusing measurement. These sets of Monte Carlo simulated rates were computed in such a way as to reproduce the corresponding experimental moments and covariance matrices. These rates were then fed into the code that calculates the efficiencies and activities. The ESTAR stopping powers were used and *kB* was fixed at 0.0075 cm/MeV. The standard deviation of the distribution of the activities thus generated was assumed to be the propagation of the rates' pdfs on the activity.

The last and main component is that of reproducibility, computed here as the relative standard deviation of four activities obtained with the four sources from two solutions. The combined relative standard uncertainty obtained from the quadratic sum of these contributions is 0.74%.

3.3. Reference ionisation chamber measurements

The measurements of the currents produced in the reference ionisation chamber by the M177Lu4 solution in the IER, ISO and BIPM ampoules are shown in Fig. 10. Good agreement is found between the measurements of each ampoule type. The average normalised current is 15.053(5) pA/g for IER ampoules, 15.237(6) pA/g for ISO ampoules and 14.974(6) pA/g for BIPM ampoules. The differences between these values are explained by the different geometry of the ampoule types, their glass wall thicknesses and their filling level.

Using these currents and the activity concentration obtained from the primary measurements, a calibration factor, called equivalent activity A_e, can be calculated for the CIR for each ampoule type. It was determined that A_e IER = 293.71(130) (0.44%) MBq, A_e BIPM = 295.21 (131) (0.44%) MBq and A_e ISO = 290.24(129) (0.44%) MBq.

For the second dilution M177Lu5, with ampoule types IER and ISO, a good agreement is also found between the measurements and the average normalised current is 1.0550(15) pA/g and 1.0670(17) pA/g respectively. Using these values and the one obtained for the dilution M177Lu4, one can calculate a dilution factor of 14.270(21) from IER ampoules and 14.280(24) from ISO ampoules. These two values are well compatible and are in good agreement with the gravimetric dilution factor 14.262(2) within the uncertainties.

4. Discussion

The activity concentration determined by 4πβ-4πγ coincidence measurements using plastic scintillators for beta detection and analogue electronics presented an excellent internal consistency. The activity ratio of the M177Lu4 solution over that of the M177Lu5 solution agreed within 0.04%.

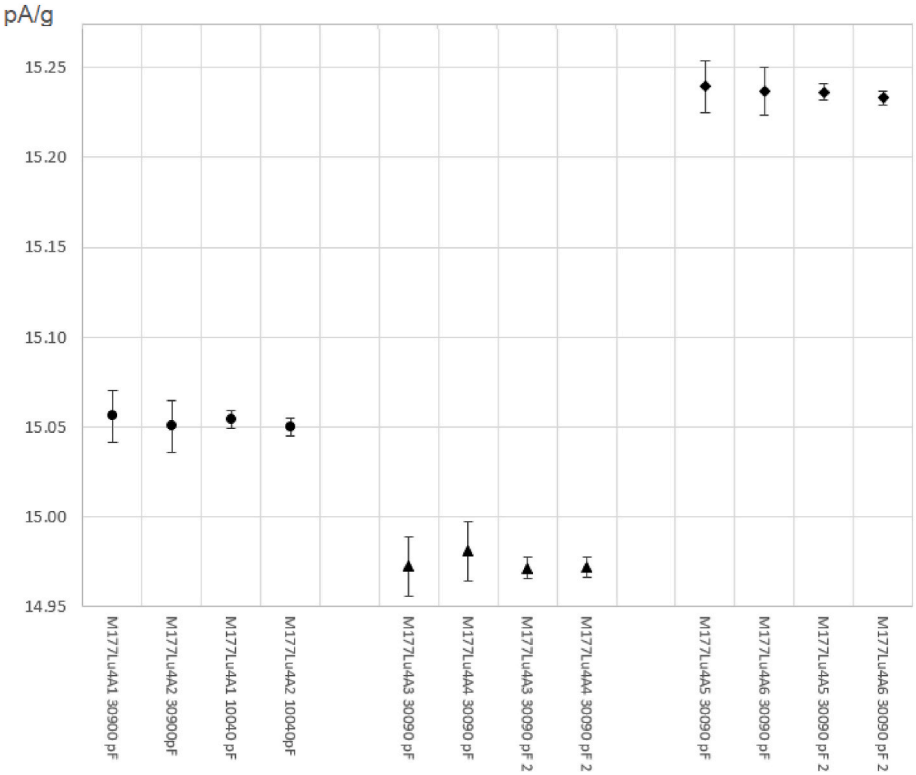

Fig. 10. Current values measured with the CIR in pA/g for each of the three ampoule types (IER in circles, BIPM in triangles, and ISO in diamonds). Each ampoule is measured two times. The largest uncertainties for the two first measurements stem from the propagation of the half-life uncertainty. They were measured five days before the reference date compared to 1 day for the other measurements.

This activity concentration agreed well with those predicted by 4πβ-4πγ or 4πβ-γ coincidence measurements using digital electronics, though the proper functioning of the digitizer and its software are yet to be fully validated and the extrapolation functions exhibited an unexplained non-linear behaviour, which is being examined.

However, the 4πβ-4πγ measurement with analogue electronics predicts an activity concentration that is 1.8% smaller than that determined using the TDCR method. Using allowed form factors instead of first-forbidden form factors for the Geant4 beta spectra of the first forbidden transitions, as did (Kossert et al., 2012), does not significantly change this discrepancy. It must also be noted that these limited TDCR measurements did not show the robust internal consistency they usually have. Furthermore, this discrepancy is all the more surprising because for ^{161}Tb, which has a similar decay scheme to that of ^{177}Lu, there was a very good agreement between the 4πβ(PS)-4πγ coincidence technique and the TDCR method.

One year after the measurements, a colleague suggested that the source of the discrepancy may be some pure beta emitting or electron capture impurity. To investigate this possibility, two samples from the fully decayed M177Lu4 solution were prepared using the same procedure discussed in section 2.2.2, and then measured for 40 h each on the Wallac 1220 Quantulus^{TM} spectrometer. No long-lived impurity was found. There might have been some short-lived pure beta emitting impurity at the time of the standardisation, but we did not check for such impurities at the time. However, with regard to long-lived impurities such as tritium, no such evidence was found.

In any case, similar discrepancies between the coincidence counting with solid sources and liquid scintillation measurements were reported in the international comparison for the activity measurement of ^{177}Lu, the IRMM obtained a deviation of 3.3% between its coincidence measurement with a proportional counter and its CIEMAT-NIST measurement, while the NPL found 0.8% for this difference (Zimmerman et al., 2012). Note however that the PTB reported a very close agreement between these determinations (0.03%).

An ampoule of the M177Lu4 solution was sent to the BIPM as a submission to the *Système International de Référence*. The activity concentration complementing the contribution was calculated as the average of the analogue plastic coincidence counting activity determinations, i.e. the mean of twelve efficiency-extrapolated activities obtained with four sources, from two dilutions, with degrees of freedom ranging from 31 to 38. It was estimated to be 5862.76 kBq g^{-1}, with a total relative standard uncertainty of 0.41%. The digital β-γ coincidence determinations were not included in this mean, notwithstanding their agreement with their analogue counterparts, because the operation of our DT5725 digitizer and its software are yet to be fully validated. We did not include the TDCR result in the average because it did not display its expected robust internal coherence.

5. Conclusion

To back up the use of ^{177}Lu for targeted radionuclide therapy, a solution of this nuclide provided by ITM GmbH was standardised using coincidence counting, with plastic scintillation in the beta channel, as well as the TDCR method. The solution had no detectable trace of ^{177m}Lu or other gamma-emitting impurity.

The 4πβ(PS)-4πγ coincidence measurements showed high beta detection efficiencies but relatively low efficiencies in the gamma channel, in part because of the low-intensity low-energy gamma emissions of ^{177}Lu. Linear efficiency functions were found for all the gamma settings, though for sources prepared with Ludox a slight departure from linearity was observed at small inefficiencies. These coincidence-counting measurements were found to be self-consistent and mutually compatible.

The 4πβ(PS)-4πγ and 4πβ(PS)-γ coincidence measurements with digital electronics showed a satisfactory internal coherence and agreed with each other. The analogue and digital coincidence counting activity concentrations agreed within standard uncertainties. However, the β-γ coincidence measurements were found to be 1.8% lower than the TDCR determination.

An ampoule of the standardised solution was dispatched to the BIPM as a submission to the *Système International de Référence*.

CRediT authorship contribution statement

Youcef Nedjadi: Writing – review & editing, Writing – original draft, Validation, Methodology, Investigation, Formal analysis, Data curation, Conceptualization. **Frédéric Juget:** Writing – original draft, Validation, Investigation, Formal analysis, Conceptualization. **M. Teresa Durán:** Writing – review & editing, Validation, Methodology, Investigation, Formal analysis, Conceptualization. **Laurent Desorgher:** Writing – review & editing, Software, Investigation, Formal analysis. **François Bochud:** Writing – review & editing, Supervision, Resources, Funding acquisition. **Claude Bailat:** Writing – review & editing, Supervision, Resources, Project administration, Funding acquisition, Conceptualization.

Declaration of competing interest

The authors declare that they have no known competing financial interests or personal relationships that could have appeared to influence the work reported in this paper.

Data availability

No data was used for the research described in the article.

References

Allison, J., et al., 2006. Geant4 developments and applications. IEEE Trans. Nucl. Sci. 53, 270–278.

Allison, J., et al., 2016. Recent developments in Geant4. Nucl. Instrum. Methods A835, 186–225.

Berger, M.J., 1993. ESTAR, PSTAR and ASTAR, a PC Package for Calculating Stopping Powers and Ranges of Electrons, Protons and Helium Ions. IAEA-NDS-144.

Bouchard, J., Cassette, P., 2000. MAC3: an electronic module for the processing of pulses delivered by a three photomultiplier liquid scintillation counting system. Appl. Radiat. Isot. 52, 669–672.

Bouchard, J., Chauvenet, B., 1999. A simple, powerful 4πβ–γ coincidence system based on the pulse-mixing method. Nucl. Instrum. Methods A 422, 395–399.

Capogni, M., Cozzella, M.L., De Felice, P., Fazio, A., 2012. Comparison between two absolute methods used for ^{177}Lu activity measurements and its standardization. Appl. Radiat. Isot. 70, 2075–2080.

Champion, C., Quinto, M.A., Morgat, C., Zanotti-Fregonara, P., Hindié, E., 2016. Comparison between three promising ß-emitting radionuclides, ^{67}Cu, ^{47}Sc and ^{161}Tb, with emphasis on doses delivered to minimal residual disease. Theranostics 6, 1611–1618.

Dias, M.S., Silva, F.F.V., Koskinas, M.F., 2010. Standardization and measurement of gamma-ray probability per decay of ^{177}Lu. Appl. Radiat. Isot. 68, 1349–1353.

Dryák, P., Sochorová, J., Šolc, J., Auerbach, P., 2016. Activity standardization, photon emission probabilities and half-life measurements of ^{177}Lu. Appl. Radiat. Isot. 109, 160–163.

Grau Malonda, A., Grau Carles, A., 1999. The ionization quench factor in liquid-scintillation counting standardizations. Appl. Radiat. Isot. 51, 183–188.

Gümüş, H., Kabadayi, Ö., 2010. Practical calculations of stopping powers for intermediate energy electrons in some elemental solids. Vacuum 85, 245–252 and private communication.

Kellett, M.A., 2016. '177Lu: DDEP Evaluation of the decay scheme for an emerging radiopharmaceutical'. Appl. Radiat. Isot. 109, 129–132.

Kossert, K., Nähle, O.J., Ott, O., Dersch, R., 2012. Activity determination and nuclear decay data of ^{177}Lu. Appl. Radiat. Isot. 70, 2215–2221.

Lehenberger, S., Barkhausen, C., Cohrs, S., Fischer, E., Grünberg, J., Hohn, A., Köster, U., Schibli, R., Türler, A., Zhernosekov, K., 2011. The low-energy β- and electron emitter 161Tb as an alternative to ^{177}Lu for targeted radionuclide therapy. Nucl. Med. Biol. 38, 917–924.

Nedjadi, Y., Bailat, C., Bochud, F., 2012. Primary activity measurements with a 4πβ-4πγ coincidence counting system. Appl. Radiat. Isot. 70, 249–256.

Nedjadi, Y., Bailat, C., Caffari, Y., Cassette, P., Bochud, F., 2015. Set-up of a new TDCR counter at IRA-METAS. App. Radiat. and Isot. 97, 113–117.

Nedjadi, Y., Duc, P.-F., Bochud, F., Bailat, C., 2016. On the stability of ^{3}H and ^{63}Ni Ultima Gold liquid scintillation sources. Appl. Radiat. Isot. 118, 25–31.

Nedjadi, Y., Laedermann, J.-P., Bochud, F., Bailat, C., 2017. On the reverse micelle effect in liquid scintillation counting. Appl. Radiat. Isot. 125, 94–107.

Nedjadi, Y., Juget, F., Desorgher, L., Durán, M.T., Bochud, F., Müller, C., Talip, Z., van der Meulen, N.P., Bailat, C., 2020. Activity standardisation of ^{161}Tb. Appl. Radiat. Isot. 166, 109411.

Rezende, E.A., Correia, A.R., Iwahara, A., da Silva, C.J., Tauhata, L., Poledna, R., da Silva, R.L., de Oliveira, E.M., de Oliveira, A.E., 2012. Radioactivity measurements of ^{177}Lu, ^{111}In and ^{123}I by different absolute methods. Appl. Radiat. Isot. 70, 2081–2086.

Schötzig, U., Schrader, H., Schönfeld, E., Günther, E., Klein, R., 2001. Standardisation and decay data of ^{177}Lu and ^{188}Re. Appl. Radiat. Isot. 55, 89–96.

Simpson, B.R.S., van Staden, M.J., Lubbe, J., van Wyngaardt, W.M., 2012. Accurate activity measurement of Lu-177 by the liquid scintillation 4πβ–γ coincidence counting technique. Appl. Radiat. Isot. 70, 2209–2214.

Talip, Z., Juget, F., Ulrich, J., Nedjadi, Y., Buchillier, T., Durán, M.T., Bochud, F., Bailat, C., van der Meulen, N., 2021. Determination of the gamma and X-ray emission intensities of Erbium-169. Appl. Radiat. Isot. 176, 109823.

Tan, Z., Xia, Y., 2012. Stopping power and mean free path for low-energy electrons in ten scintillators over energy range of 20–20 000 eV. Appl. Radiat. Isot. 70, 296–300.

Zimmerman, B.E., Altzitzoglou, T., Antohe, A., Arinc, A., Bakhshandeiar, E., Bergeron, D. E., Bignell, L., Bobin, C., Capogni, M., Cessna, J.T., Cozzella, M.L., da Silva, C.J., De Felice, P., Dias, M.S., Dziel, T., Fazio, A., Fitzgerald, R., Iwahara, A., Jaubert, F., Johansson, L., Keightley, J., Koskinas, M.F., Kossert, K., Lubbe, J., Luca, A., Mo, L., Nähle, O., Ott, O., Paepen, J., Pommé, S., Sahagia, M., Simpson, B.R.S., Silva, F.F.V., van Ammel, R., van Staden, M.J., van Wyngaardt, W.M., Yamazaki, I.M., 2012. Results of an international comparison for the activity measurement of ^{177}Lu. Appl. Radiat. Isot. 70, 1825–1830.